

Variational multiscale nonparametric regression: Algorithms

Miguel del Alamo^{1,†}, Housen Li^{2,†}, Axel Munk^{2,*} and Frank Werner^{3,†}

¹ Department of Applied Mathematics, University of Twente

² Institute for Mathematical Stochastics, University of Göttingen

³ Institute of Mathematics, University of Würzburg

Abstract

Many modern statistically efficient methods come with tremendous computational challenges, often leading to large scale optimization problems. In this work we examine such computational issues for modern estimation methods in nonparametric regression with a specific view on image denoising. We consider in particular variational multiscale methods which are statistically optimal in minimax sense, yet computationally intensive. The computation of such a multiscale Nemirovski Dantzig estimator (MIND) requires to solve a high dimensional convex optimization problem with a specific structure of the constraints induced by a multiple statistical multiscale testing criterion. To solve this, we discuss three different algorithmic approaches: The Chambolle-Pock, ADMM and semismooth Newton algorithms. Explicit implementation is presented and the solutions are then compared numerically in a simulation study and on various test images. We thereby recommend the Chambolle-Pock algorithm in most cases for its fast convergence.

Keywords: Non-smooth large-scale optimization; image denoising; variational estimation; multiscale methods, MIND estimator.

MSC: 62G05, 68U10.

1 Introduction

In this paper we consider the nonparametric regression (a.k.a. denoising) problem, that is to estimate the unknown function $f : [0, 1]^d \rightarrow \mathbb{R}$ given noisy observations

$$Y_i = f(x_i) + \sigma \epsilon_i, \quad x_i \in \Gamma_n, \quad i = 1, \dots, n, \quad (1)$$

where ϵ_i are independent normal random variables with zero mean and unit variance, and Γ_n is a discrete grid in $[0, 1]^d$ that consists of n points. We stress that much of what is addressed in this paper can be generalized to other error models. However, to keep the presentation simple we restrict ourselves to the Gaussian error and equidistant grids in the d -dimensional unit

*Correspondence: munk@math.uni-goettingen.de.

†These authors contributed equally to this work.

cube. A mathematical theory of such nonparametric regression problems has a long history in statistics (see [63] for an early reference), as they are among the simplest models where the unknown object is still in a complex function space and not just encoded in a low-dimensional parameter, yet they are general enough to cover many applications (see e.g. [27]). Consequently, nonparametric regression is a relatively well-understood problem for which plenty of methods have been proposed, such as kernel smoothing [52, 66], global regularization techniques such as penalized maximum likelihood [25], ridge regression - which amounts to Tikhonov regularization [55, 50] or total variation (TV) regularization [60]. These methods have not been designed a priori in a spatially adaptive way which could be overcome by a second generation of (sparse) localizing regularization methods originating in the development of wavelets [13]. To fine tune the estimator for first generation methods usually a simple regularization parameter has to be chosen (statistically), for wavelet based estimators this amounts to properly select (and truncate) the wavelet coefficients methods, e.g. by soft thresholding, see e.g. [20]. We refer to [64] for an introduction to the modern statistical theory of nonparametric regression, mainly from a minimax perspective. One of the latest developments to the problem of recovering the function f in (1) already dates back to Nemirovski [53] and is implicitly exemplified by the Dantzig selector [9], that can be seen as a hybrid between a sparse approximation with respect to a dictionary and variational (L^1) regularization. Such hybrid methods have been coined in [32] as MIND estimators (MultiScale Nemirovski-Dantzig) and are the focus of this paper. We will discuss these mainly in the context of statistical image analysis ($d = 2$), but stress that our findings also apply to signal recover $d = 1$ and to other situations where multiscale approaches are advantageous, e.g. for temporal-spatial imaging, where $d = 3, 4$.

1.1 Variational denoising

One of the most prominent regularization methods for image analysis is total variation (TV) denoising, which was popularized by Rudin, Osher and Fatemi [60]. For further developments towards a mathematical theory for more general variational methods, see e.g. [61] and the references given there. In the spirit of Tikhonov regularization, the rationale behind is to enforce certain properties for the function f fitted to the model (1), which are encoded by a convex penalty term R such as the TV seminorm. Consequently, the weighted sum of a least-squares data fidelity term (corresponding to the maximum likelihood estimation in model (1)) and R is minimized over all functions g (e.g. of bounded variation), and the minimizer is taken as the reconstruction or estimator for f , i.e.

$$\hat{f} \in \arg \min_g \left[\frac{1}{2} \sum_{i=1}^n (Y_i - g(x_i))^2 + \alpha R(g) \right] \quad (2)$$

with a weighting factor (sometimes called the *regularization parameter*) $\alpha > 0$. As soon as R is convex, algorithmically, this leads to a convex optimization problem, which can be solved efficiently in practice. This also applies to other convex data fidelity, e.g. when the likelihood comes from an exponential family model. To solve (2) numerically, most common are first order methods, see e.g. [4], which boil down to computing the (sub-)gradients of the least-squares term and R .

One of the statistical disadvantages of methods of the form (2) is the usage of the global least-squares term, which to some extent enforces the same smoothness of g everywhere on the domain Γ_n . To overcome this issue, a spatially varying choice of the parameter α has been discussed in case of R being the TV seminorm, see e.g. [39, 38]. Other options are localized least-squares fidelities ([37, 19, 18]) or anisotropic total variation penalties, where the weighting matrix A is also improved iteratively based on the available data (see e.g. [45]). We will discuss another powerful strategy to cope with local inhomogeneity of the signal which has its origin in statistics and has been recently shown to be statistically optimal (in a certain sense to be made precise below) for various choices of penalties R .

1.2 Statistical multiscale methods

In the nonparametric statistics literature, multiscale methods have their origin in the discovery of wavelets [13], which Donoho and Johnstone [23] used to construct wavelet thresholding estimators and showed their ability to adapt to certain smoothness classes. Such estimators are computationally simple, as they only involve thresholding with respect to an orthonormal basis (cf. [20]). Following wavelets, a myriad of multiscale dictionaries tailored to different needs have been developed, such as curvelets [7], shearlets [43], etc. In a nutshell, the superiority of multiscale dictionaries over other bases for denoising and inverse problems lies in their excellent approximation and localizing properties, which yields sparse approximations of functions w.r.t. loss functions which results from norms which average the error, e.g. L^p , $p \geq 1$, Sobolev or Besov norms. However, it is well known that despite this sparseness these estimators tend to present Gibbs-like oscillatory artifacts in statistical settings (which is not well reflected by such norms). This affects the quality of the overall reconstruction critically [8, 14].

1.3 Variational mutliscale methods

Variational mutliscale methods offer a solution to the problem of such Gibbs-artifacts, as they combine multiscale methods with classical (non-sparse) regularization techniques, with the idea of making use of the best of both worlds: the stringent data-fitting properties of (overcomplete) multiscale dictionaries, and the desired (problem dependent) smoothness imposed by a regularization method, e.g. by TV regularization.

Definition 1. Let \mathcal{F} be a class of functions, $R : \mathcal{F} \rightarrow \mathbb{R} \cup \{\infty\}$ a convex functional, and $\{\phi_\lambda | \lambda \in \Lambda_n\}$ a finite collection of functions. Given observations Y_i as in (1), the Multiscale Nemirovski-Dantzig Estimator (MIND) is defined by the constrained optimization problem

$$\hat{f} \in \underset{g \in \mathcal{F}}{\operatorname{argmin}} R(g) \quad \text{s.t.} \quad \max_{\lambda \in \Lambda_n} |\langle \phi_\lambda, g - Y \rangle| \leq q_n \quad (3)$$

for a threshold $q_n > 0$, where we use the inner product $\langle h, g \rangle := n^{-1} \sum_{i=1}^n h(x_i)g(x_i)$.

Several particular cases of the MIND have been proposed: the first time by Nemirovski [53] (who gives credit to S. V. Shil'man) in 1985 for a system of indicator functions and a Sobolev seminorm $R(g) = |g|_{H^s}$, Donoho [20] derived soft-thresholding from this principle where the dictionary $\{\phi_\lambda | \lambda \in \Lambda_n\}$ is a wavelet basis. Fo the latter see also [48]. For the case of a

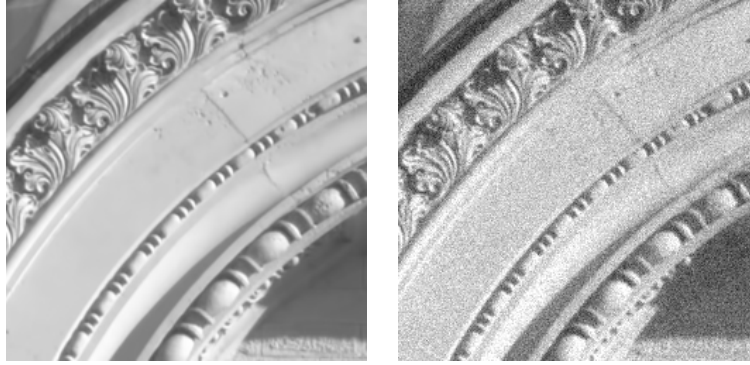
curvelet frame we refer to [8], and for a system of indicator functions and the Poisson likelihood to [29, 30] where $R(g) = |g|_{BV}$ is the TV seminorm. Notice that in practice, the choices of R and the dictionary reflect previous knowledge or expectations on the unknown function f : the amount of regularization that R imposes should be dependent on how smooth we expect f to be; and the dictionary should measure patterns that we expect f to obey, e.g. elongated features in case of curvelets, piecewise constant areas in case of indicator functions. Furthermore, we have the following rule of thumb: the more redundant the dictionary, the better the statistical properties of the estimator but the more expensive the computation of a solution to (3).

It is documented that the different proposed instances of the MIND show increased regularity and reduced artifacts as compared with standard multiscale methods (i.e. thresholding type estimators), but still avoid oversmoothing if the threshold q_n is appropriately chosen, see [29, 30, 14]. For instance, we illustrate in Figure 1 that the MIND with R the TV seminorm outperforms the soft-thresholding estimator under various choices of multiscale dictionaries, including wavelets, curvelets and shearlets. In addition to their good empirical performance, estimators of the form (3) have recently been analyzed theoretically and proved to be (nearly minimax) optimal for nonparametric regression [32, 14] and certain inverse problems [9, 15]. We will give a brief review of these theoretical results in Section 2.

1.4 Computational challenges and scope of the paper

However, the practical and theoretical superiority of regularized multiscale methods over purely dictionary thresholding methods comes at a cost: instead of simple thresholding, a complex optimization problem has to be solved, with an increase in computation time and the need of improved optimization methods. In practice, the problem (3) is non-smooth (e.g. if R is chosen as the TV seminorm), and is furthermore high-dimensional due to a huge number of constraints. For instance, in case of images of 256×256 pixels, the number of constraints is 1,751,915 for the dictionary of cubes of edge length ≤ 30 and 3,211,264 for that of shearlets.

Besides our theoretical review in Section 2, the goal of this paper is to discuss different particularly successful algorithmic approaches for the solution of (3) in Section 3. Among the first attempts is the usage of the alternating direction method of multipliers (ADMM) in [28, 29, 30], including a problem-specific convergence analysis. The computational disadvantage of this approach is the necessity to compute projections to the constraint set, which is most generally done by Dykstra's algorithm. Even though this can be efficiently implemented using GPUs (cf. [44, 42]), the projection step provides a computational bottleneck of the overall algorithm. Several other convex optimization algorithms such as Douglas-Rachford-Splitting (see [49]) or the Proximal Alternating Predictor Corrector algorithm (cf. [47]) also require the computation of such projections, and hence their computational performance is similar to the ADMM-based version. In view of this, we will furthermore discuss two new approaches based on the Chambolle-Pock algorithm [11] on the one hand and a semismooth Newton method (cf. [Hintermüller, 12]) on the other. The former allows to avoid computing projections to the constraint sets, but requires only the computation of the corresponding resolvent operator, which reduces to a high-dimensional soft-thresholding problem. The latter allows to solve a regularized version of the optimality conditions by Newton's method and then apply a path-continuation scheme to decrease the amount of regularization. Both algorithms hence avoid



(a) Truth

(b) Noisy image, PSNR=23.5



(c) MIND, wavelets, PSNR=25.3



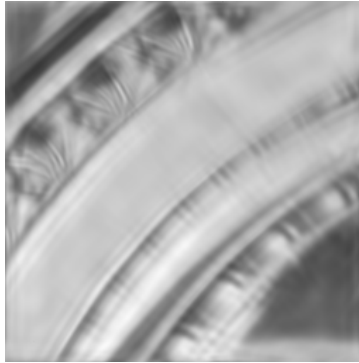
(d) MIND, curvelets, PSNR=25.8



(e) MIND, shearlets, PSNR=27.4



(f) ST, wavelets, PSNR=24.1



(g) ST, curvelets, PSNR=23.9



(h) ST, shearlets, PSNR=24.6

Figure 1: Comparison of MIND with TV regularization and the soft-thresholding (ST) estimator on the “building” image from Darmstadt Noise Dataset [56] with different dictionaries. Details of dictionaries can be found in Section 4.2. The thresholds for MIND and ST are chosen the same as the 50% quantile of $\|\sigma\epsilon\|_{MS}$ in (5), see Section 2.2.

Dykstra’s projection step, but still have favorable convergence properties.

In Section 4 we will finally discuss the practical advantages and disadvantages of the previously described algorithms along different numerical examples. For all examples checked in this paper, we found that the Chambolle-Pock algorithm is superior compared to the others. Finally, we provide a Matlab implementation of the Chambolle-Pock algorithm for this problem and code to run all examples in <https://github.com/housenli/MIND>.

2 Theoretical properties of variational multiscale estimation methods

In this section we briefly review some theoretical reconstruction properties of multiscale variational estimators within model (1). Recall that in the nonparametric regression model (1), we have access to noisy samples of a function f at locations $x_i \in \Gamma_n$. We have some flexibility in choosing the underlying grid Γ_n : it could be for instance an equidistant d -dimensional grid (e.g. as pixels in an image), but other choices are possible (e.g. a polar grid).

2.1 Theoretical guarantees

Estimators of the form (3) have been analyzed from a theoretical viewpoint in a variety of settings. When the dictionary basis functions ϕ_λ are orthogonal this becomes particular simple, as then the evaluation functionals (if the truth equals g) $\langle \phi_\lambda, \epsilon \rangle$ become independent in model (3). This is valid for wavelet systems and their statistical analysis is vast, see e.g. [46, 22, 21, 67, 34, 5, 68, 1, 6] for various forms of adaptation and thresholding techniques. If the dictionary is redundant the analysis becomes more difficult (see, however, [33] for the asymptotic validity of hard and soft thresholding in this case) and only in recent years it could be shown that suitably constructed MINDs with redundant dictionaries perform optimal in a statistical (minimax) sense over certain function spaces.

- *Sobolev spaces*: [53] and [32] analyzed the MIND with $R(g) = |g|_{H^s}$ and $\{\phi_\lambda\}$ being a set of indicator functions of rectangles at different locations and scales. They showed that, for the choice $q_n = C \sigma \sqrt{\log n/n}$ for an explicit constant $C > 0$, the MIND is minimax optimal up to logarithmic factors for estimating functions in the Sobolev space H^s . This means that the MIND’s expected reconstruction error is of the same order as the error of the best possible estimator, i.e.

$$1 \leq \frac{\sup_{|f|_{H^s} \leq L} \mathbb{E} \|f - \hat{f}_{MIND}\|_{L^p}}{\inf_{\text{all estimators } \hat{f}} \sup_{|f|_{H^s} \leq L} \mathbb{E} \|f - \hat{f}\|_{L^p}} \leq C \text{Polylog}(n). \quad (4)$$

Besides minimax optimality, [32] also showed that the MIND with H^s regularization is also optimal for estimating functions in other Sobolev spaces H^t for certain smoothness indices t , a phenomenon known as adaptation.

- *Bounded variation*: In [14], the MIND with bounded variation regularization $R(g) = |g|_{BV}$ was considered. It was shown that it is optimal in a minimax sense up to logarithms for

estimating functions of bounded variation if $d = 2$. For $d \geq 3$ the discretization matters further and this could only be shown in a gaussian white noise model. Such results hold for a variety of dictionaries $\{\phi_\lambda\}$, such as wavelet bases, mixed wavelet and curvelet dictionaries, and suitable systems of indicator functions of rectangles as well.

In addition to theoretical guarantees, these results also provide a way of choosing the threshold parameter q_n in (3). Indeed, both for Sobolev and for bounded variation regularization, it is shown (see again [32, 14]) that the choice $q_n = C \sigma \sqrt{\log n/n}$ for an explicit constant $C > 0$ yields asymptotically optimal performance. The constant C depends on the dimension d and smoothness s of the functions, on whether we consider Sobolev or BV regularization, and on the dictionary $\{\phi_\lambda\}$ we employ.

2.2 Practical choice of the threshold q_n

Besides the theoretically (asymptotically) optimal choice of the parameter q_n , a Monte Carlo method for a finite sample choice was proposed in [32]. It is based on the observation that the multiscale constraint in (3) can be interpreted as a test statistic for testing whether the data Y is compatible with the function g , in the sense of (1). In fact, the "multiscales" come from not only performing one test, but many tests that focus on different features of g of various sizes, locations and orientations. From this viewpoint, q_n is interpreted as a critical value for a statistical test, and statistical testing theory suggests that q_n should be chosen as a high quantile of the random variable

$$\|\sigma\epsilon\|_{\text{MS}} := \sigma \max_{\lambda \in \Lambda_n} |n^{-1} \sum_{i=1}^n \epsilon_i \phi_\lambda(x_i)|. \quad (5)$$

This interpretation yields a practical way of choosing q_n : We simply pre-estimate σ , simulate independent realizations of the noise ϵ , compute their values in (5), and finally set q_n to be a quantile of that sample. This choice of q_n yields good practical performance (see Section 4) and is compatible with the theoretically optimal choice for n large enough. Methods for pre-estimating σ from the data can be found in [51].

3 Computational methods

In this section, we will discuss different algorithmic approaches to compute the MIND \hat{f} in (3). First of all, we stress that the optimization problem (3) is a non-smooth, convex, high dimensional optimization problem, which allows in principle to exploit any optimization method designed for such situations. In the following we restrict to three different approaches, which we found particular suited for our scenario. To set the notation in this section, we rewrite (3) as

$$\min_{v \in \mathbb{R}^n} J(v), \quad J(v) := F(Kv) + G(v), \quad (6)$$

where F and G are lower semi-continuous, proper convex functionals given by

$$\begin{aligned} F(w) &:= 1_{\leq 0}(w - KY - q_n) + 1_{\leq 0}(-w + KY - q_n) \quad \text{for } w \in \mathbb{R}^{\#\Lambda_n}, \\ G(v) &:= R(v) \quad \text{for } v \in \mathbb{R}^n. \end{aligned}$$

and K is the linear (bounded) operator that maps from \mathbb{R}^n to $\mathbb{R}^{\#\Lambda_n}$ and is defined by

$$[Kg_n]_\lambda := \langle \phi_\lambda, g_n \rangle \quad \text{for any } \lambda \in \Lambda_n.$$

Here and in what follows, $1_{\leq 0}$ denotes the indicator function of the negative half-space, this is

$$1_{\leq 0}(v) = \begin{cases} 0 & v_i \leq 0 \text{ for all possible } i, \\ \infty & \text{else.} \end{cases}$$

Due to the convexity of F and G , the problem (6) can equivalently be solved by finding a root of the subdifferential $\partial J(v)$ (see e.g. [59]), which is a generalization of the classical derivative. Such roots correspond to stationary points of the evolution equation

$$\partial v(t) \in -\partial J(v(t)), \quad t > 0.$$

Two fundamental algorithms for the solution of this equation arise from applying the explicit or implicit Euler method, which leads to the method of steepest decent

$$v_{k+1} \in (I - \lambda_k \partial J)(v_k), \quad k \in \mathbb{N} \quad (7a)$$

and the so-called proximal point method

$$v_{k+1} \in (I + \lambda_k \partial J)^{-1}(v_k), \quad k \in \mathbb{N} \quad (7b)$$

respectively, where I denotes the identity operator and $\lambda_k > 0$ is a step size parameter. The operator $(I + \lambda_k \partial J)^{-1}$ is a so-called resolvent operator, the computation of which is clearly as difficult as the original problem. However, motivated by the two methods different algorithms have been suggested. Therefore, the subdifferential $\partial J(v)$ of J is split into the subdifferentials of F and G , which allow for a much simpler computation of the corresponding resolvent operators. This makes use of the formula

$$\partial J(v) = K^* \partial F(Kv) + \partial G(v), \quad (8)$$

which holds true whenever there exists some vector $v \in \mathbb{R}^n$ such that both F and G are finite and continuous at Kv and v respectively (see e.g. Prop. 5.6 in [26]). In our situation, this is the case whenever R is continuous at a point in the interior of the feasible set. With the help of (8) we can also derive the necessary and (due to convexity) sufficient first-order optimality conditions

$$-K^*w \in \partial G(v), \quad (9a)$$

$$Kv \in \partial F^*(w) \quad (9b)$$

with the conjugate functional

$$F^*(w) := \sup_{v \in \mathbb{R}^n} \left[w^\top v - F(v) \right].$$

In the following, we present three different algorithms to solve (6) either via a specific splitting of ∂J or via the first-order optimality conditions: the Chambolle-Pock primal dual algorithm, an ADMM method, and a semismooth Newton method.

3.1 The Chambolle-Pock method

The primal dual algorithm by Chambolle and Pock [11] is based on a reformulation of the optimality conditions (9) as fixed point equations. If we multiply the second condition by a parameter $\tau > 0$ and add w on both sides yields

$$w + \tau K v \in w + \tau \partial F^*(w).$$

Similarly, the first condition yields

$$v - \delta K^* w \in v + \delta \partial G(v).$$

Hence, the solutions v and w of the optimality conditions can be found by repetitively applying the resolvent operators of G and the dual of F , which are given by

$$(I + \tau \partial G)^{-1}(v) := \operatorname{argmin}_{x \in \mathbb{R}^n} \frac{\|x - v\|^2}{2\tau} + R(v) \quad (10a)$$

$$(I + \delta \partial F^*)^{-1}(w) := \operatorname{argmin}_{z \in \mathbb{R}^{\#\Lambda_n}} \frac{\|z - w\|^2}{2\delta} + q_n \sum_{\lambda \in \Lambda_n} |z_\lambda - \delta Y_\lambda|. \quad (10b)$$

This combined with an extrapolation step yields the Chambolle-Pock algorithm. It can also be interpreted as a splitting of the subdifferential ∂J into those of F and G , and then applying proximal point steps (i.e. backwards steps) to ∂G and the dual of ∂F .

The first proximal operator in (10) depends on the regularizing functional $R(\cdot)$, which is typically convex, so the computation can be done efficiently. For instance, it can be solved by quadratic programming [54] if $R(\cdot)$ is a Sobolev norm, and with Chambolle's algorithm [10] if $R(\cdot)$ is the TV penalty.

The second proximal operator in (10) involves the high-dimensional constraint. However, the solution to (10b) is simply the soft-thresholding operator applied to $\delta^{-1}w - KY$ with threshold $q_n \delta$. Altogether, the Chambolle-Pock algorithm applied to (3) is given in Algorithm 1.

Algorithm 1: Chambolle-Pock algorithm

Require: $\delta, \tau > 0$, $\theta \in [0, 1]$, $k = 0$, $(v_0, w_0) \in X \times Y$, stopping criterion

- 1: **while** stopping criterion not satisfied **do**
 - 2: $w_{k+1} \leftarrow (I + \delta \partial F^*)^{-1}(w_k + \delta K \tilde{v}_k)$
 - 3: $v_{k+1} \leftarrow (I + \tau \partial G)^{-1}(v_k - \tau K^* w_{k+1})$
 - 4: $\tilde{v}_{k+1} \leftarrow v_N + \theta(v_{k+1} - v_k)$
 - 5: $k \leftarrow k + 1$
 - 6: **end while**
 - 7: **Return** (v_k, w_k)
-

In order to run the Chambolle-Pock algorithm, we need to choose the step sizes δ and τ , and convergence of the algorithm is ensured whenever $\tau\delta \leq \|K\|_{op}^{-2}$. Due to the different difficulty of the two subproblems, it is reasonable to choose $\delta \neq \tau$ and, in particular, to choose $\delta > \tau$. More precisely, the subproblem with respect to F is more involved because of the large number of constraints, so this requires a much smaller step size, which by the Moreau's identity is equivalent to choosing a much larger δ . We observe in practice that the choices $\delta = \|K\|_{op}^{-1}\sqrt{n}$ and $\tau = \|K\|_{op}^{-1}/\sqrt{n}$ yield good results, see Section 4.

We remark that, in the Chambolle-Pock method applied to this problem, the high-dimensionality appears only in the very simple problem of soft-thresholding. This is a very convenient way of dealing with it and, as we will see, will make the Chambolle-Pock-algorithm superior over the ADMM method.

3.2 ADMM method

The alternating direction methods of multipliers (ADMM) can be seen as a variant of the augmented Lagrangian method, see [58, 35] for classical references. To derive it, we introduce a slack variable $h \in \mathbb{R}^{\#\Lambda_n}$ and rewrite (3) it into the equivalent problem

$$\operatorname{argmin}_{v \in \mathbb{R}^n, w \in \mathbb{R}^{\#\Lambda_n}} F(w) + G(v) \quad \text{subject to } Kv = w.$$

By the convex duality theory, it is equivalent to find the saddle point of the augmented Lagrangian $L_\lambda(v, w; h)$, that is,

$$\operatorname{argmin}_{v, w} \max_{h \in \mathbb{R}^{\#\Lambda_n}} F(w) + G(v) + \langle h, Kv - w \rangle + \frac{\lambda}{2} \|Kv - w\|^2$$

where $h \in \mathbb{R}^{\#\Lambda_n}$ is the Lagrangian multiplier, and $\lambda > 0$. As its name suggests, the ADMM algorithm solves this saddle point problem alternately over v, w and h in a Gauß-Seidel fashion (i.e. successive displacement). The details are given in Algorithm 2 below.

The usage of the ADMM for the problem (3) was first proposed by [29]. One central difference compared to the Chambolle-Pock algorithm is that the ADMM splitting avoids the usage of F^* . Instead, it deals with the high-dimensional constraint in an explicit way, which ultimately results in a slower performance.

From the steps performed by the ADMM in Algorithm 2, the first one (line 2) involves the proximal operator of R and can typically be dealt with with a standard algorithm (see the discussion in the Chambolle-Pock algorithm, Section 3.1). The second step (line 3) is more challenging, as it involves solving the optimization problem

$$w_k = \operatorname{argmin}_w \frac{\lambda}{2} \|w - (Kv_k + \lambda^{-1}h_{k-1})\|^2 \quad \text{subject to } \max_{\lambda \in \Lambda_n} |w_\lambda - \langle \phi_\lambda, Y \rangle| \leq q_n. \quad (11)$$

In other words, we have to find the orthogonal projection of the point $Kv_N + \lambda^{-1}h_{N-1}$ to the feasible set

$$\{w \in \mathbb{R}^{\#\Lambda_n} \mid \max_{\lambda \in \Lambda_n} |w_\lambda - \langle \phi_\lambda, Y \rangle| \leq q_n\}.$$

This set is the intersection of $2\#\Lambda_n$ half-spaces, and it is known to be non-empty (as it always contains $\{Y, \phi_\lambda\} | \lambda \in \Lambda_n\}$). The projection problem (11) can be solved by Dykstra's algorithm [24, 3], which converges linearly [17]. See [2] for an efficient stopping rule.

Finally, it follows from Corollary 3.1 in [16] that the ADMM has a linear convergence guarantee for the problem (6).

Algorithm 2: Alternating direction method of multipliers (ADMM)

Require: data $Y \in \mathbb{R}^n$, step size $\lambda > 0$, tolerance $\epsilon > 0$, initial values v_0, w_0, h_0

- 1: **while** $\max\{\|Kv_k - w_k\|, \|K(v_k - v_{k-1})\|\} > \epsilon$ **do**
 - 2: $v_k = \operatorname{argmin}_v \frac{\lambda}{2} \|Kv - (w_{k-1} - \lambda^{-1}h_{k-1})\|^2 + G(v)$
 - 3: $w_k = \operatorname{argmin}_w \frac{\lambda}{2} \|w - (Kv_k + \lambda^{-1}h_{k-1})\|^2 + F(w)$
 - 4: $h_k = h_{k-1} + \lambda(Kv_k - w_k)$
 - 5: $k \leftarrow k + 1$
 - 6: **end while**
 - 7: **Return** (v_k, w_k)
-

3.3 Semismooth Newton method

Besides the optimality conditions (9), the problem (3) can also be solved by the so-called Karush-Kuhn-Tucker conditions, which are necessary and sufficient as well. Using the notation of this section, the original problem (3) is equivalent to

$$\min_{v \in \mathbb{R}^n} R(v) \quad \text{s.t.} \quad q_n - Kv + KY \geq 0, q_n - KY + Kv \geq 0. \quad (12)$$

This is a convex optimization problem with linear inequality constraints, and if we introduce $B : \mathbb{R}^n \rightarrow \mathbb{R}^{2\#\Lambda_n}$ as $v \mapsto Bv$ with $B = (K^\top, -K^\top)^\top$, then a vector v is a solution to (12) if and only if there exists a vector of Lagrange multipliers $\lambda \in \mathbb{R}_{\geq 0}^{2\#\Lambda_n}$ such that

$$\partial R(v) \ni -B^\top \lambda, \quad (13a)$$

$$q_n - Bv + BY \geq 0, \quad (13b)$$

$$\lambda_i (q_n - Bv + BY)_i = 0 \quad \text{for all } 1 \leq i \leq 2\#\Lambda_n. \quad (13c)$$

The latter two conditions can be reformulated as

$$\lambda_i = \max\{0, \lambda_i + c(Bv - BY - q_n)_i\} \quad \text{for all } 1 \leq i \leq 2\#\Lambda_n. \quad (14)$$

The immediately visible advantage of this formulation over the original problem is that the inequality constraints have been transformed into equations. Now suppose for a moment that

the functional R is twice differentiable. Then $\partial R(v)$ is single valued and (13a) is a differentiable equation for v and λ . It seems a natural approach to solve the corresponding system of equations (13a) and (14) via an analog of Newton's method. On the other hand, even if R was twice differentiable, the max function in (14) is not differentiable in the classical sense. The application of Newton's method is however still possible, as the max function turns out to be semismooth (see Definition 2.5 in [Hintermüller]). For a general operator B , it is however not clear if the overall system (13a) and (14) can also be described as finding the root of a semismooth function. Therefore, one introduces a regularization parameter $\beta \in (0, 1)$ and replace (14) by the regularized equation $\lambda_i = \beta \max\{0, \lambda_i + c(Bv - BY - q_n)_i\}$ for all $1 \leq i \leq 2\#\Lambda_n$, which is in turn equivalent to

$$\lambda_i = \max\left\{0, \frac{\beta c}{1 - \beta} (Bv - BY - q_n)_i\right\} \quad \text{for all } 1 \leq i \leq 2\#\Lambda_n. \quad (15)$$

This system is now explicit in λ and yields in combination with (13a) the overall system

$$\partial R(v) \ni -\frac{1}{\delta} B^\top \max\{0, (Bv - BY - q_n)\} \quad (16)$$

with the new regularization parameter $\delta := (1 - \beta)/(\beta c) \in (0, \infty)$. This system can – for twice differentiable R and under appropriate assumptions on B satisfied in our example – now shown to be semismooth (cf. [36]). Furthermore, for $\delta \searrow 0$, the solution of the regularized system (16) converges towards a solution of the original system (13). This follows from the fact that (15) is in fact the Moreau-Yoshida regularization of the second optimality condition (9b). In practice, this limiting process is realized by a path-continuation scheme, sustaining the superlinear convergence behavior.

For differentiable R , such as the Sobolev seminorm $R(v) = |v|_{H^s}$, the implementation of the semismooth Newton method with path-continuation is now straightforward: The overall system to be solved can now be written as

$$T_\delta(v) = 0, \quad \text{where } T_\delta = \partial|v|_{H^s} + \delta^{-1} B^\top \max\{0, Bv - BY - q_n\}. \quad (17)$$

Denote by $\mathcal{D}_k[T_\delta]$ the generalized derivative of the functional at the position u_k . Then we initialize the iteration at $\delta_0 > 0$ and $u_{0,\delta}$ and solve the linear equations

$$\mathcal{D}_k[T_\delta]u_{k+1,\delta} = \mathcal{D}_k[T_\delta]u_{k,\delta} + T_\delta(u_{k,\delta}) \quad \text{for } k \geq 0$$

iteratively until a stopping criterion is satisfied. Then the parameter δ is decreased by a fixed factor (say 1/2) and the iteration is started again with $u_{k,\delta}$ as the initial guess. This continuation process is stopped until a global error criterion is reached, which is formulated in terms of the number and magnitude of the violated constraints: see Algorithm 3 below.

In case of a non-differentiable R such as the TV-seminorm, we introduce another regularization for R , resulting in its Huber regularization

$$TV_\beta(v) = \int \min\{\beta^{-1} |\nabla v|^2, |\nabla v|\} dx.$$

This functional is differentiable for any $\beta > 0$, and to compute the limit $\beta \searrow 0$ we again apply a path-continuation strategy (cf. [12]). In this case, the superlinear convergence behavior is sustained. However, we remark that the path-following routine for two parameters (δ and β) turns out to be unstable in practice. Instead, it might be desirable to look for the Moreau-Yoshida regularization of *both* the constraint and R , that is, to regularize the optimality conditions (13) in one step with just one parameter. We leave this idea to be pursued in future work.

Finally, we remark that this superlinear convergence of the semismooth Newton method is a huge theoretical advantage over the Chambolle-Pock and the ADMM algorithms. In practice, however, the situation is more complex, as the convergence speed of Newton's method depends strongly on the initialization.

Algorithm 3: Semismooth Newton method for $R(v) = |v|_{H^s}$

Require: data $Y \in \mathbb{R}^n$, step size $\Delta\delta > 0$, tolerance $\epsilon, \delta_{\min}, \rho_{\min}, r_{\min} > 0$, initial δ

- 1: $v_{old} \leftarrow 0 \in \mathbb{R}^n$
 - 2: $ratio, res \leftarrow 1$
 - 3: **while** $\delta > \delta_{\min}$ **do**
 - 4: **while** $ratio > \rho_{\min}$ or $res > r_{\min}$ **do**
 - 5: $v_{new} \leftarrow$ solution to equation: $\nabla T_\delta(v_{old})v_{new} = \nabla T_\delta(v_{old})v_{old} - T_\delta(v_{old})$ with tolerance ϵ
 - 6: $ratio \leftarrow \frac{\#\{q_n - Bv_{new} + BY < 0\}}{2\#\Lambda_n}$
 - 7: $res \leftarrow \frac{\sqrt{\|\max\{Kv_{new} - KY - q_n, 0\}\|^2 + \|\max\{KY - q_n - Kv_{new}, 0\}\|^2}}{\|v_{new}\|}$
 - 8: **end while**
 - 9: $v_{old} \leftarrow v_{new}$
 - 10: $\delta \leftarrow \delta \cdot \Delta\delta$
 - 11: **end while**
 - 12: Return v_{old}
-

4 Numerical study

In this section, we compare the practical performance of the Chambolle-Pock, the ADMM and the semismooth Newton algorithm in computing MIND, and demonstrate the empirical performance of MIND with respect to various choices of dictionaries. We refer to e.g. [8, 28, 29, 30, 32, 42, 14] for further numerical examinations of MIND. We select in particular Sobolev H^1 and TV seminorms as the regularization functional, with the former differentiable but the latter non-differentiable, and the 50%-quantile of $\|\sigma\epsilon\|_{MS}$ in (5) as q_n for MIND. Concerning measure of

image quality, we consider the peak signal-to-noise ratio (PSNR; [41]), the structural similarity index measure (SSIM; [65]) and the visual information fidelity (VIF; [62]) criteria. The implementation in MATLAB for the Chambolle-Pock algorithm, together with code that reproduces all the following numerical examples is available at <https://github.com/housenli/MIND>.

4.1 Comparison of three algorithms

Here we compare the convergence speed of the Chambolle-Pock, the ADMM and the semismooth Newton algorithm in solving (3) or equivalently (6). We stress that the relative performance of the three algorithms remains similar over different settings. Thus, as a particular example, we choose the “cameraman” image (256×256 pixels) as the function f in model (1), and the indicator functions of dyadic (partition) system of cubes (cf. Definition 2.2 in [32]), which consists of cubes

$$\left[i2^{-\ell}, (i+1)2^{-\ell} \right] \times \left[j2^{-\ell}, (j+1)2^{-\ell} \right] \subseteq [0, 1]^2 \quad \text{for all possible } i, j, \ell \in \mathbb{N} \quad (18)$$

as the dictionary $\{\phi_\lambda | \lambda \in \Lambda_n\}$. The noise level σ is assumed to be known and is chosen such that the signal-to-noise ratio (SNR) $\max_{i=1, \dots, n} |f(x_i)| / \sigma = 30$, see Figure 2. Besides the aforementioned image quality measures, we employ objective values $R(g_k)$, (relative) constraint gaps $(\max_{\lambda \in \Lambda_n} |\langle \phi_\lambda, g_k - Y \rangle| - q_n) / q_n$, and the distance $\|g_k - g_\infty\|$ to the limit solution g_∞ to examine the evolution of iterations g_k . The limit solution g_∞ is obtained for each algorithm after a large number of iterations, that is, 3×10^4 outer iterations for the Chambolle-Pock, 3×10^3 outer iterations for the ADMM, and the largest possible number of iterations until which the path-continuation scheme remains stable for the semismooth Newton method (in the considered setup, 29 outer iterations in case of H^1 regularization). As mentioned earlier in Section 3.3, the semismooth Newton method is unstable for the case of TV regularization, which is thus not reported here. All limit solutions g_∞ are shown in Figures 3 and 4, and are visually quite the same in each figure (while MIND with TV regularization leads to a slightly better result than that with H^1 regularization). This indicates that all three algorithms are able to find the global solution of (3) to a desirable accuracy.

To reduce the burden of practitioners on parameter tuning, we set the parameters in the Chambolle-Pock (Algorithm 1) by default as $\theta = 1$, $\delta = \|K\|_{op}^{-1} \sqrt{n}$ and $\tau = \|K\|_{op}^{-1} / \sqrt{n}$ in all settings. We note that the performance of the Chambolle-Pock, which is reported later, can be further improved by fine tuning θ and δ , and possibly also by preconditioning [57], for every choice of regularization functional and dictionary. In contrast, the parameters of the ADMM and the semismooth Newton algorithm are fine tuned towards the best performance for each case. More precisely, for the ADMM, we choose $\lambda = 50$ in case of H^1 and $\lambda = 0.5$ in case of TV, and for the semismooth Newton, we choose $\delta = 1/3$ and $\Delta\delta = 1/3$ in case of H^1 . The performance of three algorithms over time is shown in Figures 5 and 6 for H^1 and TV regularization, respectively. In both cases, the Chambolle-Pock clearly outperformed the ADMM with respect to all considered criteria. The semismooth Newton algorithm, as is ensured by the theory, exhibited a faster convergence rate than the other two, but this happened only at a very late stage. Moreover, the path-continuation scheme is sensitive to the choice of parameters, and makes it difficult to decide the right stopping stage in general. In summary,



(a) Truth

(b) Noisy, PSNR=29.5

Figure 2: Image “cameraman” and its noisy version with SNR=30.



(a) Chambolle-Pock

(b) ADMM

(c) Semismooth Newton

Figure 3: Limit solutions of all three algorithms for MIND with H^1 (PSNR=30 for all) regularization after long iterations.

from a practical perspective, the overall performance of the Chambolle-Pock algorithm has been found to be superior compared to the other algorithms. We speculate, however, that a hybrid combination of the Chambolle-Pock and the semismooth Newton algorithm (switching to the semismooth Newton algorithm after a burn in period using the Chambolle Pock algorithm) might lead to further improvement.

4.2 Comparison of different dictionaries

We next investigate the choice of dictionary $\{\phi_\lambda | \lambda \in \Lambda_n\}$ and its impact on the practical performance. Five different dictionaries are considered. The first consists of the indicator functions of dyadic cubes defined in (18), and the second is composed of the indicator functions of small cubes of edge length ≤ 30 , i.e.

$$\frac{1}{n} [i, i + \ell] \times [j, j + \ell] \subseteq [0, 1]^2 \quad \text{for } \ell = 1, \dots, 30, \text{ and all possible } i, j \in \mathbb{N}.$$



(a) Chambolle-Pock

(b) ADMM

Figure 4: Limit solutions of Chambolle-Pock and ADMM algorithms for MIND with TV (PSNR=30.6 for both) regularization after long iterations. As described in the main text, the semismooth Newton method showed an unstable behavior in combination with TV regularization, and hence the result is not documented here.

The third is the system of tensor wavelets, in particular, the Daubechies’ symlets with 6 vanishing moments. The fourth is the frame of curvelets, and the last is that of shearlets, both of which are constructed using default parameters in packages CurveLab (<http://www.curvelet.org>) and ShearLab3D (<http://shearlab.math.lmu.de>), respectively. As shown in Figures 3 and 4, different algorithms lead to almost the same final result, we only report the Chambolle-Pock algorithm, due to its empirically fast convergence.

As a reflection of versatility of images, we consider three test images of different types. They are a magnetic resonance tomography image of mouse “brain”, cf. Figure 8(a), from Radiopaedia.org (rID: 67777), a “cell” image, cf. Figure 9(a), taken from [31] and a mouse “BIRN” image, cf. Figure 10(a), from cellimagelibrary.org (doi:10.7295/W9CCDB17). See Figure 1 in the Introduction for the case of a natural image “building”. All images are rescaled to 256×256 pixels via bicubic interpolation. The SNR is set to 20 over all cases, see Figure 7 for noisy images. The results on all test images are shown in Figures 8, 9 and 10. In general, the dictionary of shearlets performed the best of all, which is followed by that of curvelets, while the rest (i.e. dyadic cubes, small cubes and wavelets) had similar performance. One exception is the “cell” image, where the dictionary of indicator functions of cubes, in particular, of small cubes, was better at detecting tiny white balls, see Figure 9. This is because of the similarity of such features and the cubes at small scales in the dictionary. The average performance over 10 random repetitions measured by aforementioned image quality measures as well as mean integrated squared error (MISE)

$$\frac{1}{n} \sum_{i=1}^n (\hat{f}(x_i) - f(x_i))^2$$

is reported in Table 1, which is consistent with the virtual inspections in Figures 8, 9 and 10. As a final remark, we emphasize that the difference in performance due to the choice of dictionaries is generally negligible, but the dictionary of shearlets slightly outperforms the other choices.

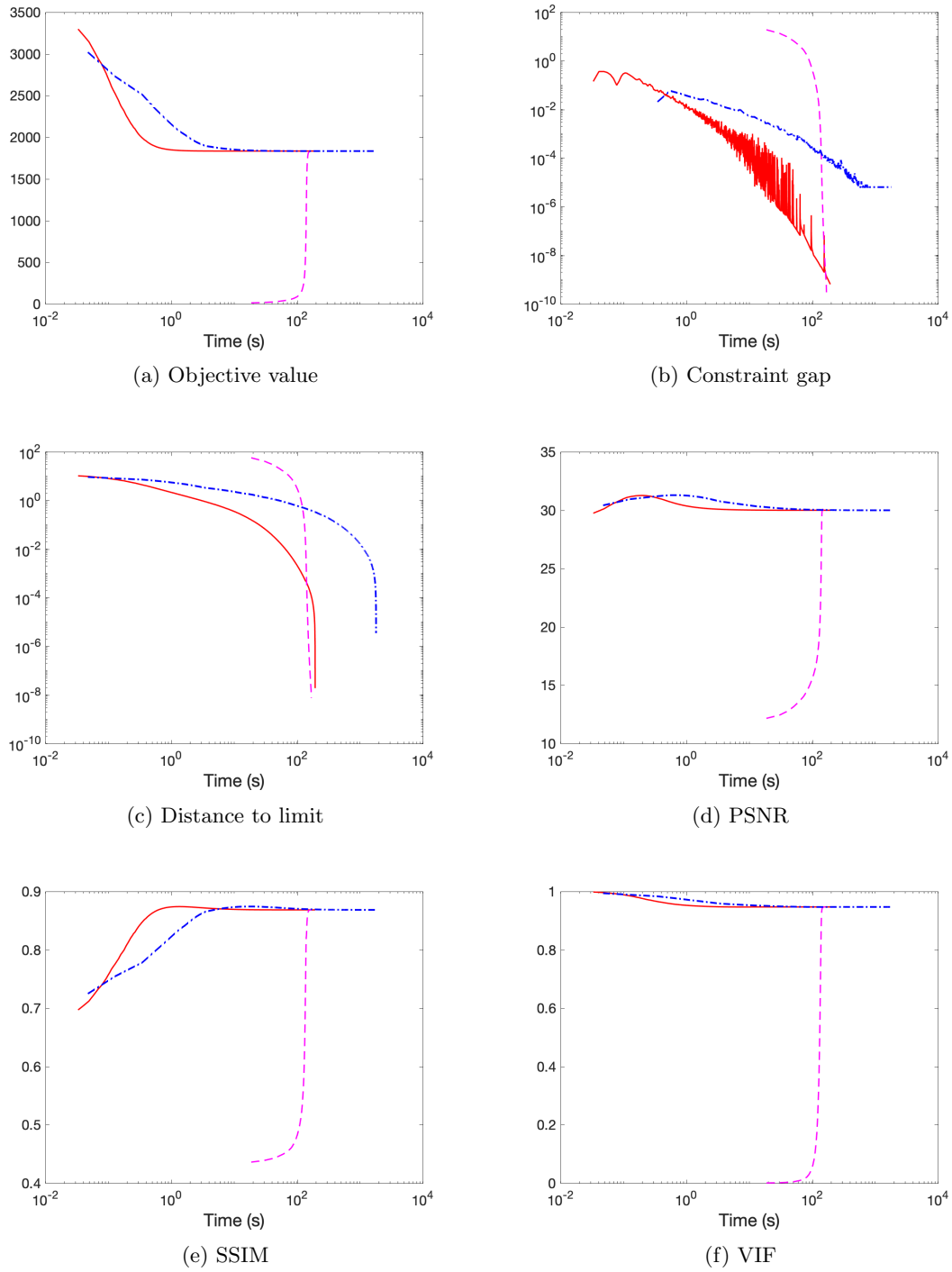
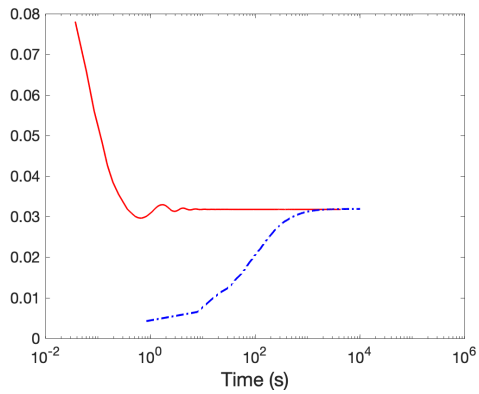
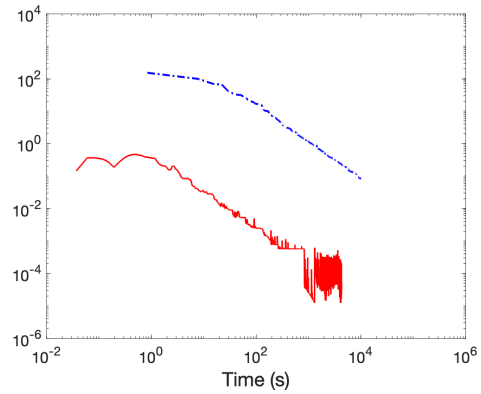


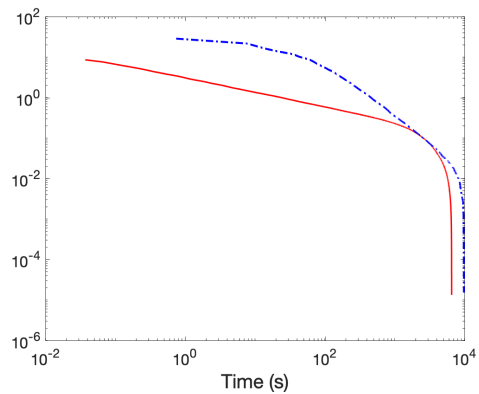
Figure 5: Performance of Chambolle-Pock (line), ADMM (dash-dot) and semismooth Newton (dash) algorithms for MIND with H^1 regularization over time.



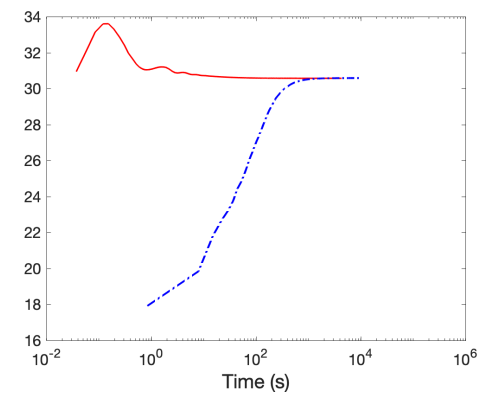
(a) Objective value



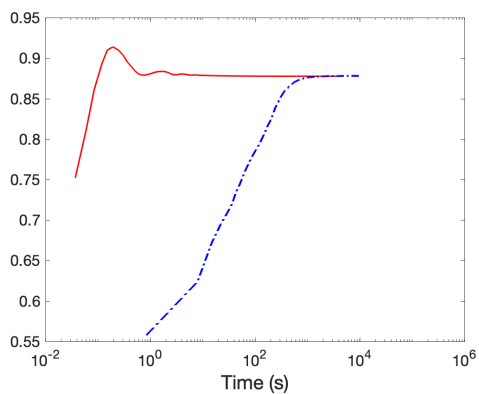
(b) Constraint gap



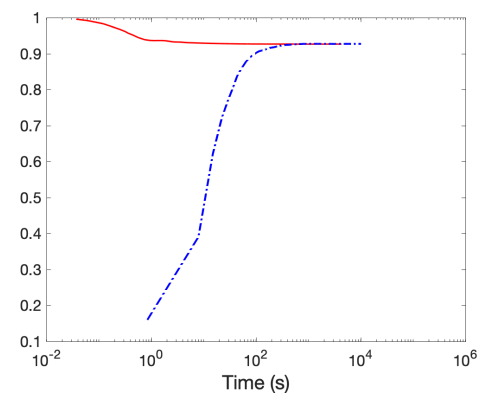
(c) Distance to limit



(d) PSNR



(e) SSIM



(f) VIF

Figure 6: Performance of Chambolle-Pock (line) and ADMM (dash-dot) algorithms for MIND with TV regularization over time.

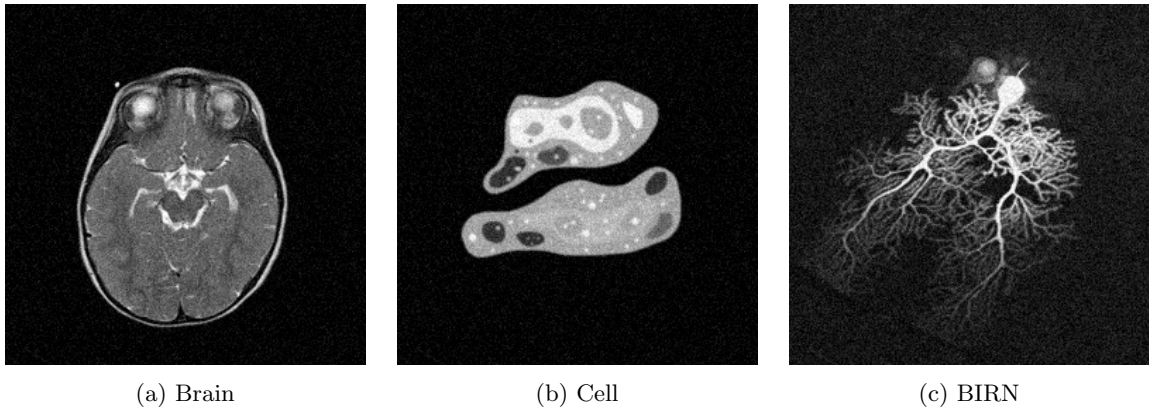


Figure 7: Noisy images of “brain”, “cell” and “BIRN” with SNR=20 and PSNR=26.

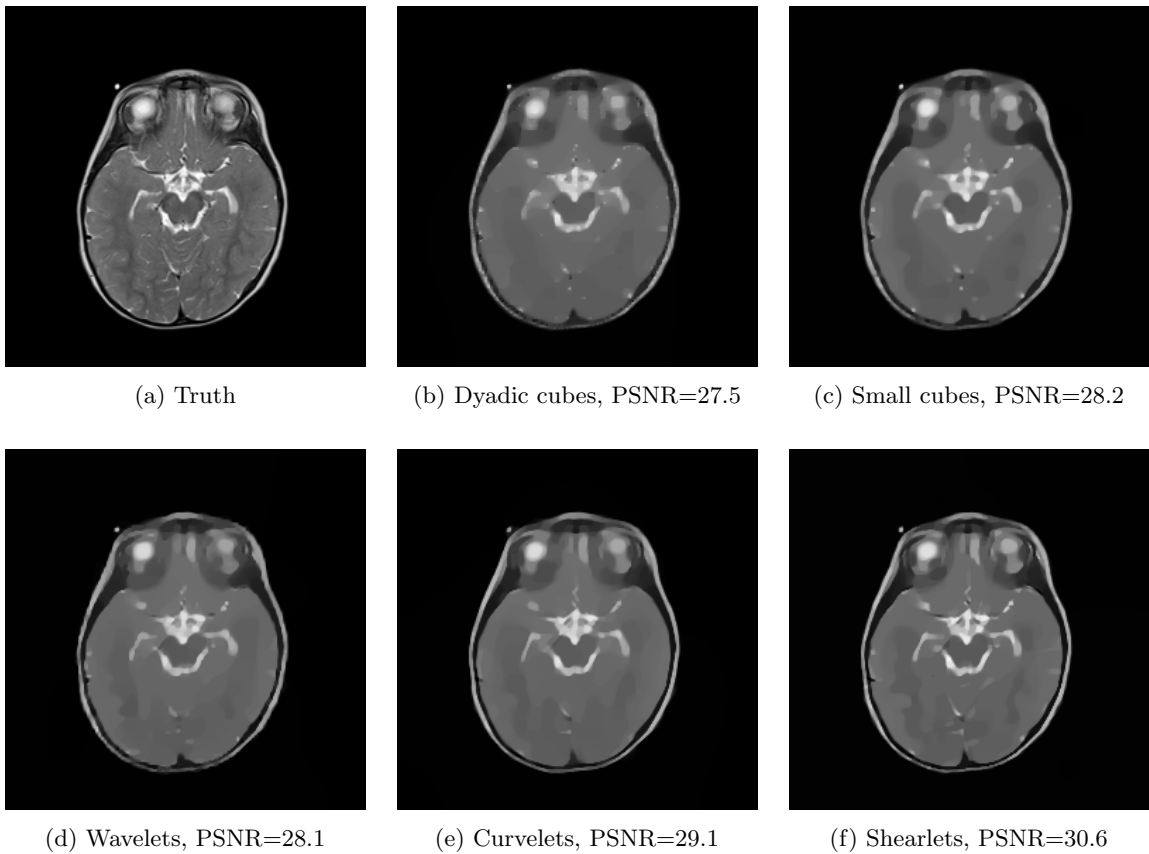


Figure 8: Results on “brain” by MIND with TV regularization and different dictionaries.

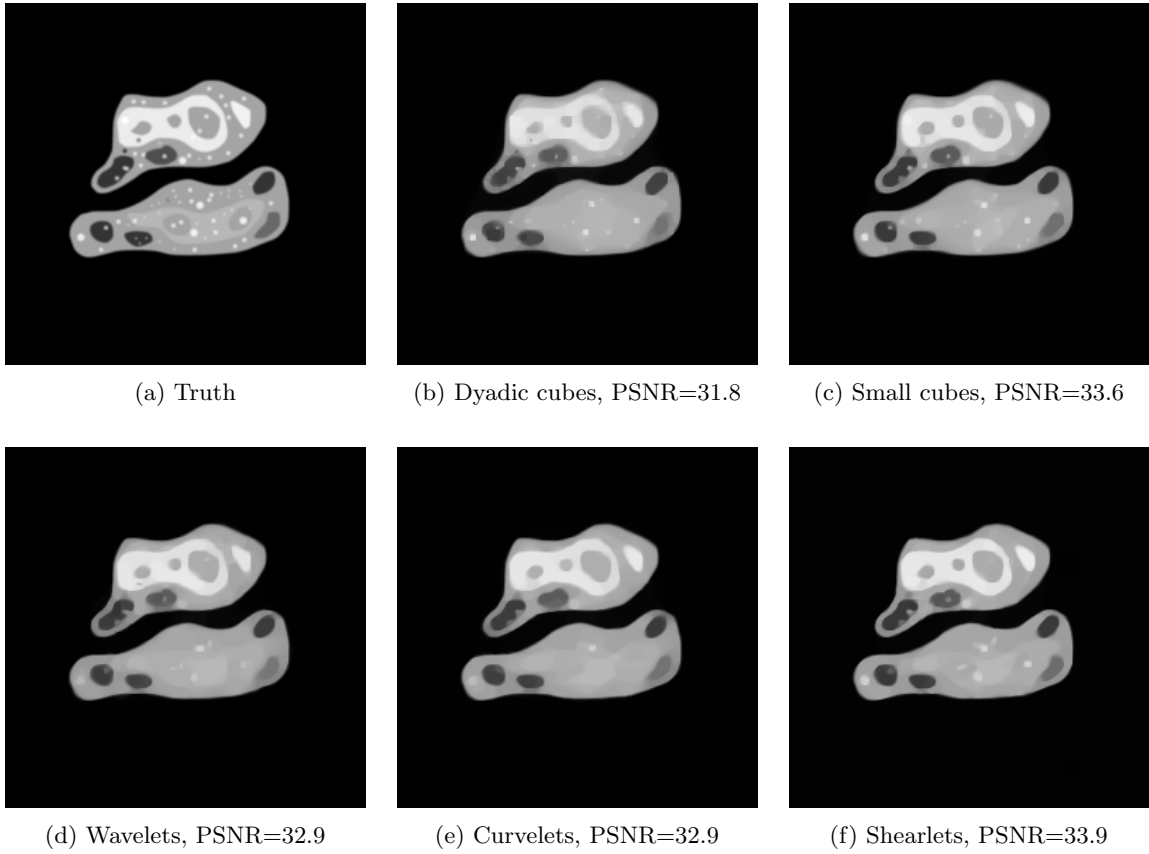


Figure 9: Results on “cell” by MIND with TV regularization and different dictionaries.

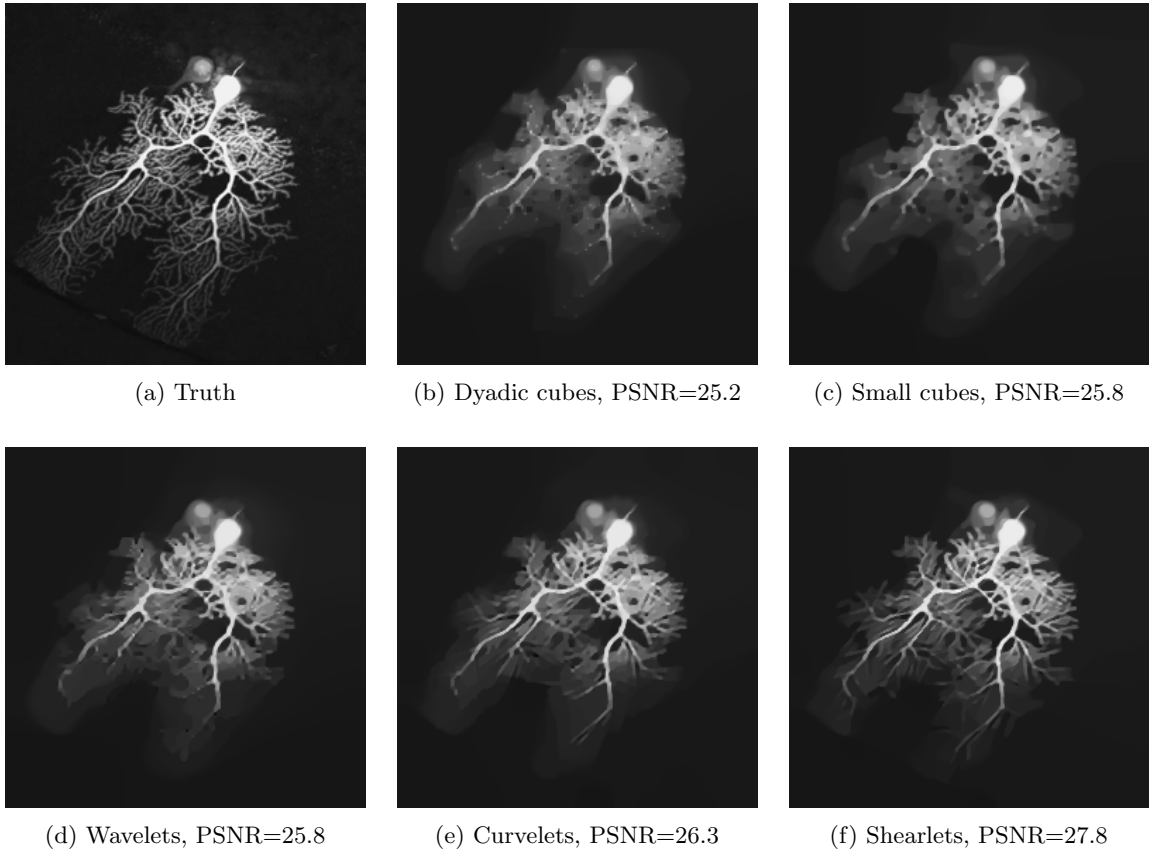


Figure 10: Results on “BIRN” by MIND with TV regularization and different dictionaries.

Table 1: Average performance of MIND with TV regularization and various dictionaries, over 10 repetitions. Values in parenthesis are standard deviations. The best value in each row is in bold.

		Dyadic cubes	Small cubes	Wavelets	Curvelets	Shearlets
"brain"	MISE	0.00176 (5.4e-06)	0.00149 (1.9e-06)	0.00147 (2.9e-05)	0.0013 (2.5e-05)	0.000871 (3e-06)
	PSNR	27.5 (0.013)	28.3 (0.0055)	28.3 (0.085)	28.9 (0.086)	30.6 (0.015)
	SSIM	0.871 (3.1e-06)	0.806 (0.002)	0.872 (0.0023)	0.852 (0.0091)	0.715 (0.0043)
	VIF	0.726 (0.00058)	0.823 (0.00036)	0.767 (0.0021)	0.809 (0.0022)	0.852 (0.00086)
"cell"	MISE	0.000671 (1.3e-06)	0.000438 (8.5e-07)	0.000509 (5e-07)	0.000554 (1.3e-05)	0.000412 (2.6e-06)
	PSNR	31.7 (0.0082)	33.6 (0.0084)	32.9 (0.0043)	32.6 (0.11)	33.9 (0.027)
	SSIM	0.912 (0.001)	0.859 (0.008)	0.924 (8.9e-05)	0.841 (0.018)	0.636 (0.0091)
	VIF	0.86 (8.2e-05)	0.913 (0.0004)	0.884 (0.0004)	0.888 (0.00057)	0.917 (0.00037)
"BIRN"	MISE	0.00301 (1.6e-06)	0.00266 (1.4e-05)	0.00269 (1e-05)	0.00237 (7.1e-06)	0.00167 (8.6e-06)
	PSNR	25.2 (0.0023)	25.7 (0.023)	25.7 (0.016)	26.2 (0.013)	27.8 (0.022)
	SSIM	0.791 (0.00012)	0.802 (0.00053)	0.81 (6.5e-05)	0.82 (0.00075)	0.858 (0.00076)
	VIF	0.718 (0.0018)	0.811 (0.0018)	0.739 (0.0024)	0.762 (0.00096)	0.838 (0.00058)

Acknowledgement

MA is supported by the Deutsche Forschungsgemeinschaft (DFG; German Research Foundation) Postdoctoral Fellowship AL 2483/1-1. HL and AM are funded by the Deutsche Forschungsgemeinschaft (DFG, German Research Foundation) under Germany's Excellence Strategy - EXC 2067/1-390729940. The authors would like to thank Timo Aspelmeier for providing code for the ADMM based implementation.

References

- [1] Abramovich, F., Benjamini, Y., Donoho, D. L., and Johnstone, I. M. (2006). Adapting to unknown sparsity by controlling the false discovery rate. *Ann. Statist.*, 34(2):584–653.
- [2] Birgin, E. G. and Raydan, M. (2005). Robust stopping criteria for dykstra's algorithm. *SIAM Journal on Scientific Computing*, 26(4):1405–1414.
- [3] Boyle, J. P. and Dykstra, R. L. (1986). A method for finding projections onto the intersection of convex sets in hilbert spaces. In *Advances in order restricted statistical inference*, pages 28–47. Springer.
- [4] Burger, M., Sawatzky, A., and Steidl, G. (2016). *First Order Algorithms in Variational Image Processing*, pages 345–407. Springer International Publishing, Cham.
- [5] Cai, T. T. (2002). On block thresholding in wavelet regression: adaptivity, block size, and threshold level. *Statist. Sinica*, 12(4):1241–1273.
- [6] Cai, T. T. and Zhou, H. H. (2009). A data-driven block thresholding approach to wavelet estimation. *Ann. Statist.*, 37(2):569–595.

- [7] Candès, E. J. and Donoho, D. L. (2000). Curvelets: A surprisingly effective nonadaptive representation for objects with edges. Technical report, Stanford University, California, Dept. of Statistics.
- [8] Candès, E. J. and Guo, F. (2002). New multiscale transforms, minimum total variation synthesis: Applications to edge-preserving image reconstruction. *Signal Processing*, 82(11):1519–1543.
- [9] Candès, E. J. and Tao, T. (2007). The dantzig selector: Statistical estimation when p is much larger than n . *The Annals of Statistics*, 35(6):2313–2351.
- [10] Chambolle, A. (2004). An algorithm for total variation minimization and applications. *Journal of mathematical imaging and vision*, 20(1):89–97.
- [11] Chambolle, A. and Pock, T. (2011). A first-order primal-dual algorithm for convex problems with applications to imaging. *Journal of mathematical imaging and vision*, 40(1):120–145.
- [12] Clason, C., Kruse, F., and Kunisch, K. (2018). Total variation regularization of multi-material topology optimization. *ESAIM: Mathematical Modelling and Numerical Analysis*, 52(1):275–303.
- [13] Daubechies, I. (1992). *Ten lectures on wavelets*, volume 61. Society for Industrial and Applied Mathematics, Philadelphia.
- [14] del Alamo, M., Li, H., and Munk, A. (2020). Frame-constrained total variation regularization for white noise regression. *To appear in The Annals of Statistics*.
- [15] del Álamo, M. and Munk, A. (2019). Total variation multiscale estimators for linear inverse problems. *Information and Inference: A Journal of the IMA*.
- [16] Deng, W. and Yin, W. (2016). On the global and linear convergence of the generalized alternating direction method of multipliers. *Journal of Scientific Computing*, 66(3):889–916.
- [17] Deutsch, F. and Hundal, H. (1994). The rate of convergence of dykstra’s cyclic projections algorithm: The polyhedral case. *Numerical Functional Analysis and Optimization*, 15(5-6):537–565.
- [18] Dong, Y., Hintermüller, M., and Rincon-Camacho, M. M. (2011a). Automated regularization parameter selection in multi-scale total variation models for image restoration. *J. Math. Imaging Vision*, 40(1):82–104.
- [19] Dong, Y., Hintermüller, M., and Rincon-Camacho, M. M. (2011b). A multi-scale vectorial L^{τ} -TV framework for color image restoration. *Int. J. Comput. Vis.*, 92(3):296–307.
- [20] Donoho, D. L. (1995). De-noising by soft-thresholding. *IEEE transactions on information theory*, 41(3):613–627.

- [21] Donoho, D. L. and Johnstone, I. M. (1995). Adapting to unknown smoothness via wavelet shrinkage. *J. Amer. Statist. Assoc.*, 90(432):1200–1224.
- [22] Donoho, D. L., Johnstone, I. M., Kerkycharian, G., and Picard, D. (1995). Wavelet shrinkage: asymptopia? *J. Roy. Statist. Soc. Ser. B*, 57(2):301–369. With discussion and a reply by the authors.
- [23] Donoho, D. L. and Johnstone, J. M. (1994). Ideal spatial adaptation by wavelet shrinkage. *Biometrika*, 81(3):425–455.
- [24] Dykstra, R. L. (1983). An algorithm for restricted least squares regression. *Journal of the American Statistical Association*, 78(384):837–842.
- [25] Eggermont, P. and LaRiccia, V. (2000). Maximum likelihood estimation of smooth monotone and unimodal densities. *Annals of statistics*, pages 922–947.
- [26] Ekeland, I. and Témam, R. (1999). *Convex analysis and variational problems*, volume 28 of *Classics in Applied Mathematics*. Society for Industrial and Applied Mathematics (SIAM), Philadelphia, PA, english edition. Translated from the French.
- [27] Fan, J. and Gijbels, I. (1996). *Local polynomial modelling and its applications: monographs on statistics and applied probability 66*, volume 66. CRC Press.
- [28] Frick, K., Marnitz, P., and Munk, A. (2012a). Shape-constrained regularization by statistical multiresolution for inverse problems: asymptotic analysis. *Inverse Problems*, 28(6):065006, 31.
- [29] Frick, K., Marnitz, P., and Munk, A. (2012b). Statistical multiresolution Dantzig estimation in imaging: fundamental concepts and algorithmic framework. *Electron. J. Stat.*, 6:231–268.
- [30] Frick, K., Marnitz, P., and Munk, A. (2013). Statistical multiresolution estimation for variational imaging: with an application in Poisson-biophotonics. *J. Math. Imaging Vision*, 46(3):370–387.
- [31] Giewekemeyer, K., Krueger, S. P., Kalbfleisch, S., Bartels, M., Salditt, T., and Beta, C. (2011). X-ray propagation microscopy of biological cells using waveguides as a quasipoint source. *Physical Review. A*, 83(2).
- [32] Grasmair, M., Li, H., and Munk, A. (2018). Variational multiscale nonparametric regression: smooth functions. In *Annales de l’Institut Henri Poincaré, Probabilités et Statistiques*, volume 54, pages 1058–1097. Institut Henri Poincaré.
- [33] Haltmeier, M. and Munk, A. (2014). Extreme value analysis of empirical frame coefficients and implications for denoising by soft-thresholding. *Applied and Computational Harmonic Analysis*, 36(3):434 – 460.

- [34] Härdle, W., Kerkycharian, G., Picard, D., and Tsybakov, A. (1998). *Wavelets, approximation, and statistical applications*, volume 129 of *Lecture Notes in Statistics*. Springer-Verlag, New York.
- [35] Hestenes, M. R. (1969). Multiplier and gradient methods. *J. Optim. Theory Appl.*, 4:303–320.
- [36] Hintermüller, M. and Kunisch, K. (2006). Path-following methods for a class of constrained minimization problems in function space. *SIAM J. Optim.*, 17(1):159–187.
- [37] Hintermüller, M., Langer, A., Rautenberg, C. N., and Wu, T. (2018). Adaptive regularization for image reconstruction from subsampled data. In Tai, X.-C., Bae, E., and Lysaker, M., editors, *Imaging, Vision and Learning Based on Optimization and PDEs*, pages 3–26, Cham. Springer International Publishing.
- [38] Hintermüller, M., Papafitsoros, K., and Rautenberg, C. N. (2017). Analytical aspects of spatially adapted total variation regularisation. *J. Math. Anal. Appl.*, 454(2):891–935.
- [39] Hintermüller, M. and Rincon-Camacho, M. (2014). An adaptive finite element method in L^2 -TV-based image denoising. *Inverse Probl. Imaging*, 8(3):685–711.
- [Hintermüller] Hintermüller, M. Semismooth newtonmethods and applications. Lecture notes for the Oberwolfach-Seminar on "Mathematics of PDE-Constrained Optimization".
- [41] Hore, A. and Ziou, D. (2010). Image quality metrics: Psnr vs. ssim. In *2010 20th international conference on pattern recognition*, pages 2366–2369. IEEE.
- [42] Kramer, S. C., Hagemann, J., Künneke, L., and Lebert, J. (2016). Parallel statistical multiresolution estimation for image reconstruction. *SIAM J. Sci. Comput.*, 38(5):C533–C559.
- [43] Labate, D., Lim, W.-Q., Kutyniok, G., and Weiss, G. (2005). Sparse multidimensional representation using shearlets. In *Wavelets XI*, volume 5914, page 59140U. International Society for Optics and Photonics.
- [44] Lebert, J., Künneke, L., Hagemann, J., and Kramer, S. C. (2015). Parallel statistical multi-resolution estimation. *arXiv preprint 1503.03492*.
- [45] Lenzen, F. and Berger, J. (2015). Solution-driven adaptive total variation regularization. In Aujol, J.-F., Nikolova, M., and Papadakis, N., editors, *Scale Space and Variational Methods in Computer Vision*, pages 203–215, Cham. Springer International Publishing.
- [46] Lepskii, O. V. (1991). On a problem of adaptive estimation in gaussian white noise. *Theory of Probability & Its Applications*, 35(3):454–466.
- [47] Luke, D. R. and Shefi, R. (2018). A globally linearly convergent method for pointwise quadratically supportable convex-concave saddle point problems. *J. Math. Anal. Appl.*, 457(2):1568–1590.

- [48] Malgouyres, F. (2002). Mathematical analysis of a model which combines total variation and wavelet for image restoration. *Journal of information processes*, 2(1):1–10.
- [49] Morken, A. F. (2017). An algorithmic framework for multiresolution based non-parametric regression. Master’s thesis, NTU.
- [50] Morozov, V. A. (1966). Regularization of incorrectly posed problems and the choice of regularization parameter. *Zhurnal Vychislitel’noi Matematiki i Matematicheskoi Fiziki*, 6(1):170–175.
- [51] Munk, A., Bissantz, N., Wagner, T., and Freitag, G. (2005). On difference-based variance estimation in nonparametric regression when the covariate is high dimensional. *Journal of the Royal Statistical Society: Series B (Statistical Methodology)*, 67(1):19–41.
- [52] Nadaraya, E. A. (1964). On estimating regression. *Theory of Probability & Its Applications*, 9(1):141–142.
- [53] Nemirovski, A. (1985). Nonparametric estimation of smooth regression functions. *Izv. Akad. Nauk. SSR Teckhn. Kibernet*, 3:50–60.
- [54] Nesterov, Y. and Nemirovsky, A. (1994). Interior-point polynomial methods in convex programming, volume 13 of. *Studies in applied mathematics*.
- [55] Phillips, D. L. (1962). A technique for the numerical solution of certain integral equations of the first kind. *Journal of the ACM*, 9(1):84–97.
- [56] Plotz, T. and Roth, S. (2017). Benchmarking denoising algorithms with real photographs. In *Proceedings of the IEEE conference on computer vision and pattern recognition*, pages 1586–1595.
- [57] Pock, T. and Chambolle, A. (2011). Diagonal preconditioning for first order primal-dual algorithms in convex optimization. In *2011 International Conference on Computer Vision*, pages 1762–1769. IEEE.
- [58] Powell, M. J. D. (1969). A method for nonlinear constraints in minimization problems. In *Optimization (Sympos., Univ. Keele, Keele, 1968)*, pages 283–298. Academic Press, London.
- [59] Rockafellar, R. T. (2015). *Convex analysis*. Princeton University Press.
- [60] Rudin, L. I., Osher, S., and Fatemi, E. (1992). Nonlinear total variation based noise removal algorithms. *Physica D: nonlinear phenomena*, 60(1-4):259–268.
- [61] Scherzer, O., Grasmair, M., Grossauer, H., Haltmeier, M., and Lenzen, F. (2009). *Variational Methods in Imaging*. Springer Science & Business Media.
- [62] Sheikh, H. R. and Bovik, A. C. (2006). Image information and visual quality. *IEEE Transactions on image processing*, 15(2):430–444.

- [63] Stone, C. J. (1982). Optimal global rates of convergence for nonparametric regression. *The annals of statistics*, pages 1040–1053.
- [64] Tsybakov, A. B. (2008). *Introduction to nonparametric estimation*. Springer Science & Business Media.
- [65] Wang, Z., Bovik, A. C., Sheikh, H. R., and Simoncelli, E. P. (2004). Image quality assessment: from error visibility to structural similarity. *IEEE transactions on image processing*, 13(4):600–612.
- [66] Watson, G. S. (1964). Smooth regression analysis. *Sankhyā: The Indian Journal of Statistics, Series A*, pages 359–372.
- [67] Weyrich, N. and Warhola, G. T. (1998). Wavelet shrinkage and generalized cross validation for image denoising. *IEEE Transactions on Image Processing*, 7(1):82–90.
- [68] Zhang, C.-H. (2005). General empirical Bayes wavelet methods and exactly adaptive minimax estimation. *Ann. Statist.*, 33(1):54–100.